THE JOURNAL OF BIOLOGICAL CHEMISTRY
Vol. 276, No. 2, Issue of January 12, pp. 1020–1025, 2001
Printed in U.S.A.

The Single Pore Residue Asp^{542} Determines Ca^{2+} Permeation and Mg^{2+} Block of the Epithelial Ca^{2+} Channel*

Received for publication, July 13, 2000, and in revised form, September 29, 2000
Published, JBC Papers in Press, October 16, 2000, DOI 10.1074/jbc.M006184200

Bernd Nilius‡§, Rudi Vennekens‡, Jean Prenen‡, Joost G. J. Hoenderop¶, Guy Droogmans‡, and Rene J. M. Bindels¶

From the ‡Department of Physiology, Campus Gasthuisberg, KU Leuven, Leuven B-3000, Belgium, and ¶Department of Cell Physiology, Institute of Cellular Signaling, University of Nijmegen, 6525 GA Nijmegen The Netherlands

The epithelial Ca^{2+} channel (ECaC), which was recently cloned from rabbit kidney, exhibits distinctive properties that support a facilitating role in transcellular Ca^{2+} (re)absorption. ECaC is structurally related to the family of six transmembrane-spanning ion channels with a pore-forming region between S5 and S6. Using point mutants of the conserved negatively charged amino acids present in the putative pore, we have identified a single aspartate residue that determines Ca^{2+} permeation of ECaC and modulation by extracellular Mg^{2+}. Mutation of the aspartate residue, D542A, abolishes Ca^{2+} permeation and Ca^{2+}-dependent current decay as well as block by extracellular Mg^{2+}, whereas monovalent cations still permeate the mutant channel. Variation of the side chain length in mutations D542N, D542E, and D542M attenuated Ca^{2+} permeability and Ca^{2+}-dependent current decay. Block of monovalent currents through ECaC by Mg^{2+} was decreased. Exchanging the aspartate residue for a positively charged amino acid, D542K, resulted in a nonfunctional channel. Mutations of two neighboring negatively charged residues, *i.e.* Glu^{535} and Asp^{550}, had only minor effects on Ca^{2+} permeation properties.

Transcellular Ca^{2+} transport in polarized epithelia of the kidney, intestine, and placenta is of vital importance for overall Ca^{2+} homeostasis. Recently, the rate-limiting step in this Ca^{2+} transport, the epithelial Ca^{2+} channel (ECaC),[1] was identified and implicated as the prime candidate target for hormonal control of transcellular Ca^{2+} transport in these epithelia (1–6).

We have recently analyzed ECaC in extensive electrophysiological studies using *Xenopus* oocytes and HEK293 cells heterologously expressing ECaC, which is important to understand the Ca^{2+} influx in Ca^{2+}-transporting epithelia (5–7). The functional hallmarks of ECaC comprise a constitutively activated Ca^{2+}-selective cation channel with a substantial permeability at physiological membrane potentials and a Ca^{2+}-dependent feedback regulation of channel activity including fast inactivation and slow current decay. Interestingly, ECaC becomes permeable to monovalent cations by lowering extracellular Ca^{2+} to micromolar concentrations. Under these latter conditions, the single channel conductance of ECaC is ~70 picosiemens.

ECaC is most closely, albeit still distantly, related to capsaicin receptors and the trp channel family (8–12). These channels function as Ca^{2+}-permeable cation channels and contain six putative transmembrane domains, including a pore-forming region between S5 and S6. Despite their structural similarity, these channels differ from ECaC in their mechanism of activation and some of their functional properties (8–11). The capsaicin receptors facilitate Ca^{2+} influx after receptor activation, whereas the trp channels are activated after Ca^{2+} store depletion or phospholipase C activation. ECaC has a high selectivity for Ca^{2+}, illustrated by P_{Ca}:P_{Na} values of more than 100, whereas the homologous channels display in general a less eminent Ca^{2+} selectivity. Furthermore, the current-voltage relationship of the capsaicin receptor and trp channels displays outward rectification, whereas ECaC currents show a pronounced inward rectification.

The aim of the present study was to elucidate the molecular determinants responsible for the key properties of ECaC. Only three negatively charged amino acid residues reside in the putative pore-forming region of ECaC, *i.e.* Glu^{535}, Asp^{542}, and Asp^{550}, which are potential Ca^{2+}-binding sites determining the conductive properties of this channel. Interestingly, these residues are absent in the other structurally related six transmembrane-spanning proteins, except for Glu^{535}, which is conserved in the capsaicin receptor (2, 4) and could therefore be responsible for the distinguishable features of ECaC. We have evaluated the functional role of these negatively charged residues and show that the aspartate at position 542 is crucial for the described hallmarks of ECaC. These findings are of vital importance in our understanding of how ECaC can show an exquisite Ca^{2+} selectivity that is relevant for the Ca^{2+} handling by Ca^{2+}-absorbing epithelia and might be important to understand dysfunctioning of Ca^{2+} absorption.

EXPERIMENTAL PROCEDURES

Molecular Biology—The open reading frame from rbECaC was cloned as a *Pvu*II-*Bam*HI fragment in the pCINeo/IRES-GFP vector (2, 4, 13). We used this bicistronic expression vector, pCINeo/IRES-GFP/rbECaC, to coexpress rbECaC and enhanced GFP. Mutagenesis of the amino acids at positions 535, 542, and 550 was carried out using the QuickChange™ Site-directed Mutagenesis Kit (Stratagene). The nucleotide sequences of mutants D535A, D542A, D542E, D542N, D542K, and D550A have been verified by sequencing the corresponding cDNAs.

Cell Culture and Transfection—Human embryonic kidney cells

* This work was supported by the Federal Belgian State (IUAP Nr.3P4/23), the Flemish Government (Levenslijn 7.0021.98, F.W.O. G.0118.00, GOA-7/1999, and FWO G.0136.00), the European Commission (BMH4-CT96–0602), and the Dutch Organization of Scientific Research (NWO-ALW 805–09.042). The costs of publication of this article were defrayed in part by the payment of page charges. This article must therefore be hereby marked "*advertisement*" in accordance with 18 U.S.C. Section 1734 solely to indicate this fact.

§ To whom correspondence should be addressed: Laboratorium voor Fysiologie, Campus Gasthuisberg, KU Leuven, Herestraat 49, B-3000 Leuven, Belgium. Tel.: 32-16-34-5937; Fax: 32-16-34-5991; E-mail: bernd.nilius@med.kuleuven.ac.be.

[1] The abbreviations used are: ECaC, epithelial calcium channel; trp, transient receptor potential; HEK, human embryonic kidney; GFP, green fluorescent protein; F, farad.

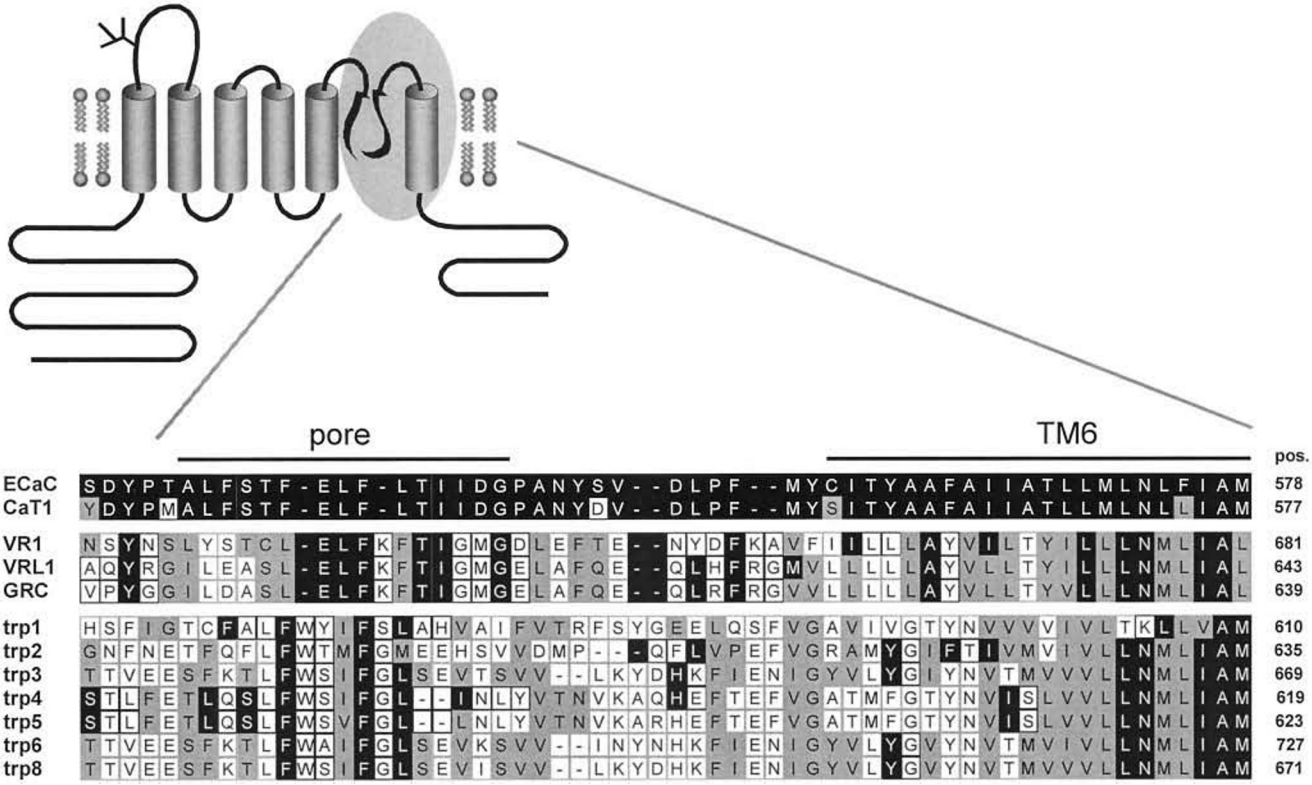

FIG. 1. **Alignment of ECaC pore region with that of homologous channels.** Identical residues are in *black boxes*, conservative substitutions are in *gray boxes*, and nonconserved amino acids are in *white boxes*. The GenBank™ accession numbers of the rabbit ECaC, rat calcium transporter 1, rat capsaicin receptor, human vanilloid receptor-like channel, mouse growth factor-regulated channel, and trp channel family are AJ133128 (rECaC), AF160798 (rCaT1), AF029310 (rVR1), AF103906 (hVRL1), AB021665 (mGRC), X89066 (htrp1), X08967 (htrp2), U47050 (htrp3), AF175406 (htrp4), AF054568 (htrp5), AF080394 (htrp6), NM00307 (htrp7), and NM012035 (mtrp8), respectively.

(HEK293) were grown in Dulbecco's modified Eagle's medium containing 10% (v/v) human serum, 2 mM L-glutamine, 2 units/ml penicillin, and 2 mg/ml streptomycin at 37 °C in a humidity-controlled incubator with 10% CO_2. HEK293 cells were transiently transfected with the pCINeo/IRES-GFP/rbECaC vector using methods described previously (14). Transfected cells were identified by their green fluorescence. GFP-negative cells from the same batch were used as controls (for details, see Ref. 14).

Electrophysiology—Electrophysiological methods and Ca^{2+} measurements have been described in detail previously (15). Electrode resistance was between 2 and 5 megaohms. Whole-cell currents were measured with an EPC-9 (HEKA Elektronik, Lambrecht, Germany) or an L/M-EPC-7 (List Elektronics, Darmstadt, Germany) using ruptured patches. Cell capacitance and access resistance were monitored continuously. The internal (pipette) solution contained 20 mM CsCl, 100 mM cesium-aspartate, 1 mM $MgCl_2$, 10 mM 1,2-bis-(2-aminophenoxy)ethane-*N,N-N′,N′*-tetraacetic acid, 4 mM Na_2ATP, and 10 mM HEPES, pH 7.2, with CsOH. The standard extracellular solution (Krebs solution) contained 150 mM NaCl, 6 mM CsCl, 1 mM $MgCl_2$, 1.5 mM $CaCl_2$, 10 mM HEPES, and 10 mM glucose, pH 7.4, with CsOH. For measuring currents carried by various monovalent cations, NaCl was equimolarly replaced by LiCl, KCl, CsCl, or *N*-metnyl-D-glucamine-Cl. For increased concentrations of Ca^{2+}, 30 mM Ca^{2+} was added to the Krebs solution. Osmotic differences were adjusted by adding the respective concentrations of mannitol to the Krebs or Ca^{2+}-free solutions. Cells were kept in a nominally Ca^{2+}-free medium to prevent Ca^{2+} overload and exposed for a maximum of 5 min to a Krebs solution containing 1.5 mM Ca^{2+} before sealing the patch pipette to the cell. All experiments were performed at room temperature (20 °C–22 °C). Stimulation protocols consisted of either linear voltage ramps from −100 or −150 mV to +100 mV within 400 ms, applied every 5 s, or step protocols consisting of a series of 60-ms voltage steps applied every 5 s from a holding potential of +20 mV to voltages between +60 and −140 or −180 mV with a decrement of 40 mV. Unless stated otherwise, the sampling interval was 1 ms for the ramp protocols and 0.2 ms for the step protocol. Data were filtered at the appropriate frequency before digitization To comparing data obtained from different cells, current amplitudes were expressed per unit of cell capacitance. We measured the permeability of different monovalent cations through ECaC by the shift in the reversal potentials of the respective ion from the reversal potentials for Na^+ currents, ΔE_{rev}, and calculated the permeability ration by

$$P_x/P_{Na} = \exp/(\Delta E_{rev} \times F/RT) \quad (1)$$

where R, T, and F have the usual meaning. The software package ASCD (G. Droogmans, Leuven, Belgium) was used for analysis of whole-cell currents including all fitting routines.

Statistical Analysis—Data are expressed as mean ± S.E. Overall statistical significance was determined by analysis of variance. In case of significance ($p < 0.01$), individual groups were compared by using Student's t test.

RESULTS

The pore region of ECaC and of the rat homologue (calcium transporter 1) contains a unique assembly of amino acids compared with the capsaicin receptors and the trp channels (Fig. 1). Most striking is the presence of three conserved negatively charged amino acids in the pore consisting of a glutamate at position 535 and aspartates at positions 542 and 550, respectively (2).

Functional Characterization of the Single Point Mutant D542A—Fig. 2 shows the effects of mutating aspartate at position 542 for alanine on the kinetics of ECaC currents during hyperpolarizing pulses. Large and stable currents were observed in cells expressing wild-type ECaC exposed to nominally Ca^{2+}-free solutions (Fig. 2*A, left panel*), which were even enhanced if extracellular Mg^{2+} was further reduced by adding 0.1 mM EDTA (Fig. 2*A, right panel*). The current induced by hyperpolarizing voltage pulses showed a fast decay to a smaller steady-state level in the presence of 1 mM Mg^{2+}, which has been described as a voltage-dependent block of ECaC by Mg^{2+} (Fig. 2*A, second panel from the left*). This block was less pronounced in the presence of both Mg^{2+} and Ca^{2+}, consistent with the permeation of Ca^{2+} through ECaC (Fig. 2*A, second*

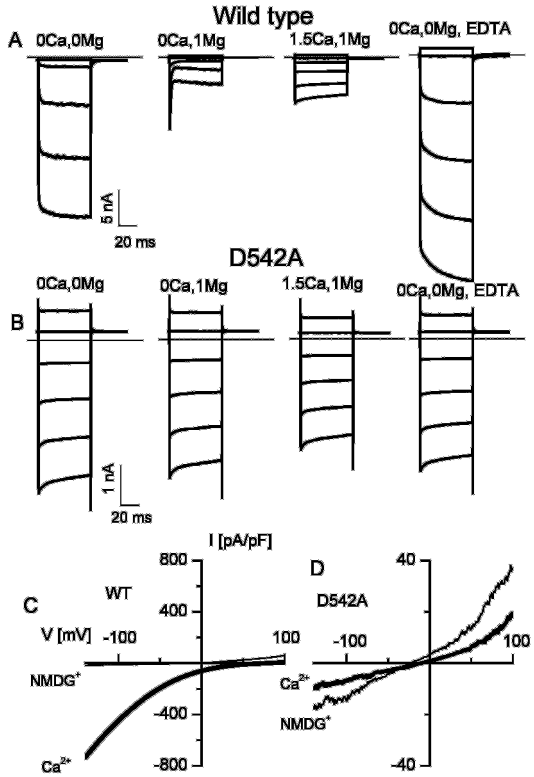

FIG. 2. **Phenotypes of the currents through wild-type ECaC and the D542A mutant channel.** Currents during voltage steps ranged from +60 mV to −140 mV (decrement, −40 mV; holding potential, +20 mV) in nominally divalent cation-free solution and solution plus either 1 mM Mg^{2+}, 1.5 mM Ca^{2+} and 1 mM Mg^{2+}, or 0.1 mM EDTA. Data were obtained from HEK cells transfected with wild-type ECaC (*A*) or D542A (*B*). *C* and *D*, currents in response to a voltage ramp protocol from −150 to +100 mV (V_H, +20 mV; duration, 400 ms). In the absence of extracellular monovalent cations (*thin line*, all substituted by *N*-metnyl-D-glucamine$^+$), administration of 30 mM Ca^{2+} (*thick line*) results in a large inward current carried by Ca^{2+} in the absence of another permeable cation. In the D542A mutant, the background current in monovalent cation-free solution was even inhibited by administration of 30 mM Ca^{2+}.

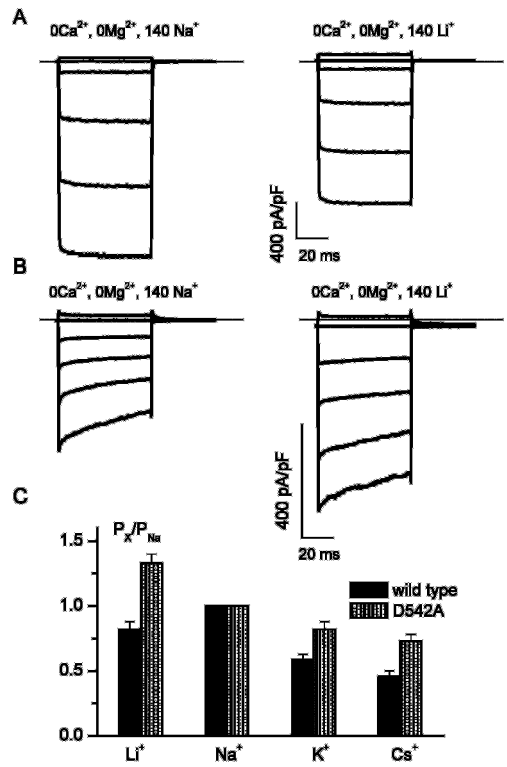

FIG. 3. **Permeation profile of monovalent cations through wild-type ECaC and the D542A mutant channel.** *A*, step responses in wild-type ECaC-transfected HEK cells (holding potential, +20 mV; steps from +60 to −140 mV; decrement, −40 mV) exposed to divalent cation-free solutions. Note that the currents carried by Na^+ are larger than those carried by Li^+, indicating an Eisenman X permeation sequence. *B*, the same protocol described in *A* was used the D542A mutant. Note that the Li^+ currents are larger than the Na^+ currents. *C*, the relative permeation was measured from the shift of the reversal potentials after substitution of Na^+ by K^+, Li^+, or Cs^+ (Eq. 1).The sequence for the D542A mutant (*gray box*) corresponds to an Eisenman XI strong field strength binding site for monovalent cations, and the sequence for wild-type ECaC (*black box*) corresponds to Eisenman X (n = 8).

panel from the right). Cells expressing the D542A mutant displayed large currents, which showed intrinsic slow inactivation. In contrast to wild-type ECaC, these currents were completely independent of extracellular Mg^{2+} and Ca^{2+} (Fig. 2*B*). The rapid current decay component due to Mg^{2+} block was absent in D542A, indicating that this mutant is insensitive to block by Mg^{2+}. This was further supported by the lack of an EDTA effect (Fig. 2*B, right panel*). A more detailed analysis revealed that the permeation pattern, estimated from the currents at −80mV normalized by the size Na^+ currents at this potential, of monovalent cations through D542A was also different from that of wild-type ECaC. The permeation sequence of wild-type ECaC was Eisenman X, with Na^+ being more permeable than Li^+ (Fig. 3*A*). D542A mutants, however, were more permeable for Li^+ than for Na^+, which is consistent with an Eisenman XI sequence (Fig. 3, *B* and *C*). The Ca^{2+} permeability of ECaC can be directly shown when Ca^{2+} is added to an extracellular solution in which all monovalent cations were substituted by *N*-methyl-D-glucamine$^+$. Under these conditions, only small currents remained, which were likely Cl^- currents. Administration of Ca^{2+} induced a large, inwardly rectifying current that reversed at very positive potentials. This current indicates Ca^{2+} influx through ECaC (16). It was completely absent in D542A. On the contrary, the background currents were even blocked in the presence of Ca^{2+} (Fig. 2, *C* and *D*). Currents through wild-type ECaC showed clear inward rectification (Fig. 4*A*), with a density of 534 ± 137 pA/pF for 30 mM Ca^{2+} at −80 mV (n = 32). The reversal potential was shifted from +15 ± 2 mV in divalent cation-free solutions (n = 21) to +47 ± 3 mV (30 mM Ca^{2+}; n = 24). For evaluation of the permeability of Ca^{2+}, we measured the difference of the reversal potential in Ca^{2+}-free solutions and in 30 mM Ca^{2+}-containing solution for all mutants tested. The absence or negative shift of the reversal potential indicates the absence of Ca^{2+} permeability. The averaged data are summarized in Fig. 4*G*. The D542A mutant did not show rectification, and current densities were smaller than those in wild-type ECaC (Fig. 4, *B* and *E*) but significantly higher than those in nontransfected HEK cells (2.5 ± 0.4 pA/pF at 30 mM Ca^{2+} and −80 mV; n = 8), indicating that the mutant is functionally expressed. Extracellular divalent cations slightly shifted the reversal potential to more negative potentials, indicating that the D542 channels are no longer permeable for divalent cations (Fig. 4*G*). The rapid and Ca^{2+}-dependent current decay during repetitive stimulations with voltage ramps, another characteristic feature of wild-type ECaC (5, 6), was abolished in the D542A mutant (Fig. 5, *A* and *B*).

Functional Effects of Mutations on Residues Neighboring Asp^{542}—Expression of the E535A and D550A mutants induced large inwardly rectifying currents (in 30 mM Ca^{2+} and at −80 mV: 151 ± 37 pA/pF (n = 8) and 87 ± 23 pA/pF (n = 7), respectively) that are not significantly different from wild-type ECaC (Fig. 4, *C* and *D*). The Ca^{2+} permeability of both mutants

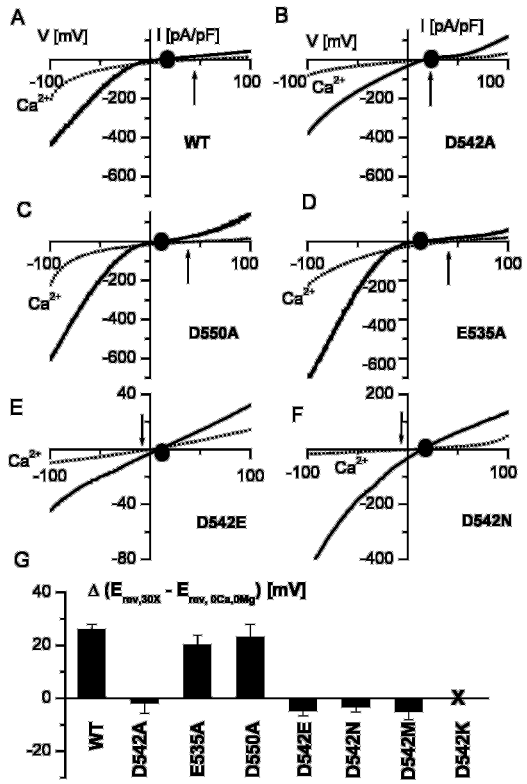

FIG. 4. **Permeation of Ca^{2+} through wild-type ECaC and mutant channels.** *A*, current-voltage relationships obtained from linear voltage ramps from −150 mV to +100 mV for wild-type ECaC in the presence of 30 mM Ca^{2+} (*dotted line*) and in divalent-free solution. Note the positive shift in reversal potential in the presence of divalent cations as well as the inward rectification. The reversal potential in the presence of 30 mM Ca^{2+} is always indicated by an *arrow*, and the reversal potential in the presence of divalent-free solution is indicated by a *solid circle*. *B*, current-voltage relationships of the mutant D542A under the same conditions as shown in *A*. Note that no obvious shift in the reversal potentials occurred in the presence of divalent cations. *C*—*F*, current-voltage relationships of the E535A, D550A, D542N, and D542E mutants, respectively, using the same protocol described in *A*. *G*, shift of the reversal potentials in the presence of 30 mM Ca^{2+}($E_{rev,30X}$) from that in the absence of divalent cations ($E_{rev,0Ca,0Mg}$), which is used as a measure of divalent permeability through ECaC (data from 6–12 cells).

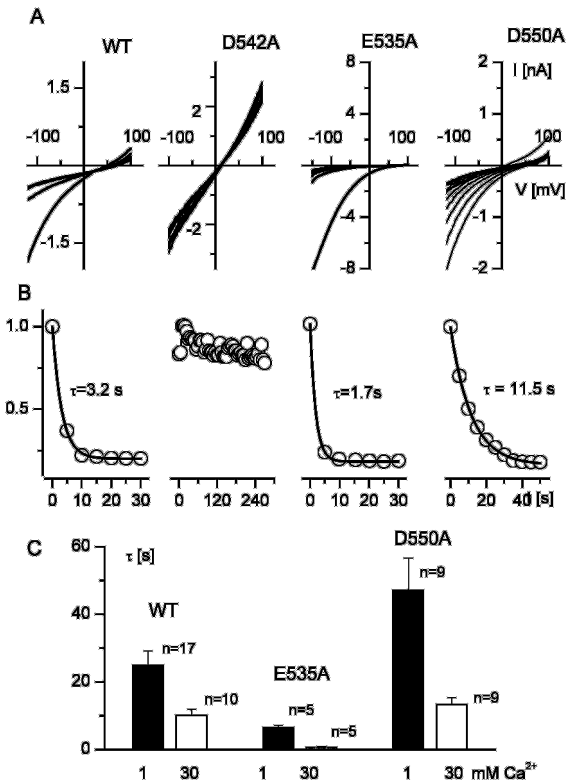

FIG. 5. **Ca^{2+}-dependent current decay in wild-type ECaC and its mutants.** *A*, current decay during repetitive voltage ramps in the presence of 30 mM Ca^{2+} (ramps range from −100mV to +100 mV; holding potential, +20 mV; interval between the ramps, 5 s) in wild-type ECaC, E535A, and D550A, but not in D542A. This decay was fitted by a monoexponential function. *B*, time course of current decay reconstructed from the normalized successive current amplitudes at −80 mV fitted to a monoexponential function. *C*, synopsis of the time constants of current decay in 1 and 30 mM extracellular Ca^{2+} concentration for the wild type (*WT*), E535A, and D550A.

was not significantly different from that of wild-type ECaC. Fig. 5 shows that currents through both mutants show a fast decay comparable to that of wild-type currents, although the rate of decay is faster for the E535A mutant and slower for the D550A mutant (Fig. 5*C*). As in the wild type, Mg^{2+} reduced the current at the end of the hyperpolarizing pulses for both the E535A and D550A mutant, with the block being more pronounced in E535A than in D550A (Fig. 6, *A, C*, and *D*).

Remodeling the Asp^{542} Residue—As shown above, the aspartate residue close to the pore is important for ECaC. A similar situation was recently described for the vanilloid receptor, in which neutralization of Asp^{646} reduced the permeability for Mg^{2+} (12). To further elucidate the role of this crucial site, we have mutated the aspartate residue by either glutamate, a negatively charged amino acid with a longer side chain, the polar asparagine, methionine with a longer side chain, and the positively charged lysine. As shown in Fig. 1, VR1, a nonselective channel that is also permeable for Ca^{2+}, has a methionine residue at the same site. Therefore, we tested this special mutant to probe whether pore characteristics similar to those for VR1 could be obtained. In addition, we have studied the permeation profile for monovalent cations through these respective mutants. Results are shown in Tables I and II. All mutants express functional cation channels. The current density is significantly increased for all mutants except D542K; the current density for D542K did not differ from that seen in nontransfected HEK cells (see Table I). D542K also showed the same permeation phenotype (data not shown) as nontransfected cells, indicating that no functional channels were expressed. However, the permeation profiles for monovalent cations were clearly different in the other mutants. In nontransfected cells, the permeation sequence follows Eisenman IV for a weak field strength site (Cs > K > Na > Li). D542M expression resulted only in very small currents with an Eisenman type IV permeation profile, also indicating a weak field strength binding site for cations that is equivalent to the background cation conductance. D542E expression also resulted in small currents, but the permeation type still matched that of a high field strength binding site as observed for wild-type ECaC and also for D542N and D542A (Table II). D542N and D542A exhibited the highest current densities for monovalent cations of all mutants. However, Ca^{2+} permeation was lacking in all mutants, as indicated by the absence of a positive shift in reversal potential on adding extracellular Ca^{2+} (Fig. 4*G*). This lack of Ca^{2+} permeation is also manifested by the absence of any current increase when 30 mM Ca^{2+} was added to a cation-free solution (same experiment as in Fig. 2, *C* and *D*; data not shown; D542A, $n = 4$; D542N, $n = 6$; D542E, $n = 4$; D542M, $n = 6$). In addition, the rapid Ca^{2+}-dependent current decay was attenuated in E, N, and M substitutions (data not shown). In contrast to D542A, the currents in the D542N and D542E mutants were inhibited by 1 mM Mg^{2+} (compare Fig. 6, *E* and *F* with Fig. 6*B*).

DISCUSSION

The present study demonstrates that a single aspartate residue located in the putative pore region of ECaC is crucial for its key features including a high Ca^{2+} permeability, block by Mg^{2+}, and Ca^{2+}-dependent current decay. These properties are essential for ECaC functioning in Ca^{2+} (re)absorption in the kidney, intestine, and placenta.

The putative pore region of ECaC contains three negatively charged amino acids that are conserved among different species (17). Our data clearly show that Asp^{542} is an important molecular determinant of Ca^{2+} selectivity and Ca^{2+} permeation through ECaC. The effects of an extension of the side chain length of this negative residue (D542E) indicate that not only the negative charge but also a steric factor controlled by the length of that side chain is important. Unexpectedly, the currents through the D542E mutants are much smaller than those for the Ala and Asn mutant. They are similar in size for the D542M mutants. D542M showed very small currents. These data, together with the permeation sequence similar to the background cation conductance, may indicate that D542M might be even nonfunctional. It is likely that the longer side chain in the D542M mutants may hinder permeation of Ca^{2+} and decrease the field strength of the monovalent binding site (Eisenman IV). Exchange of aspartate for an uncharged but polar amino acid (D542N) had similar effects, indicating that the electronegative oxygen of this side chain (at physiological pH) cannot substitute for the negative charge of aspartate. These findings indicate that both the charge and the length of the side chain at position 542 are essential for Ca^{2+} permeability.

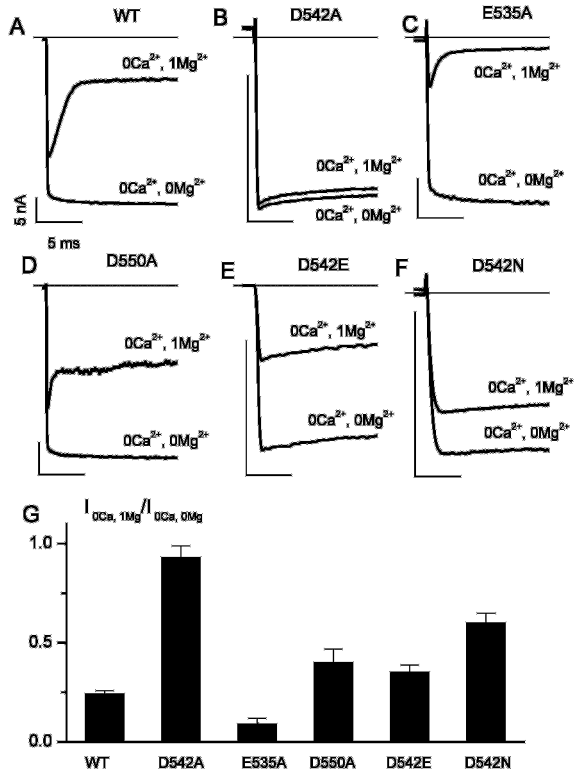

FIG. 6. **Mg^{2+} block of monovalent currents through wild-type ECaC and its mutants.** *A—F*, current responses to a hyperpolarizing voltage pulse from +20 to −140 mV in divalent cation-free solutions and in the presence of 1 mM Mg^{2+} in wild-type ECaC (*WT*), D542A, E535A, D550A, D542E, and D542N. The rapid decay compared with divalent cation-free solutions is due to voltage-dependent block of ECaC by Mg^{2+}. *G*, Mg^{2+} block was calculated as the ratio of the current at the end of the voltage pulse in 1 mM Mg^{2+} and that in the absence of divalent cations. Block is present in wild-type ECaC and in all mutants except D542A (pooled data from 5–14 cells are shown).

There is no evidence for additional negatively charged residues in the pore region. The existence of a second putative binding site for Ca^{2+} in another region of the pore is therefore unlikely. It is therefore difficult to reconcile the observed anomalous mole fraction behavior of ECaC (5) with the two-binding site model used to describe Ca^{2+} selectivity and high Ca^{2+} permeability of voltage-operated Ca^{2+} channels.

It is remarkable that substitution of aspartate at position

TABLE I

Densities of Na^+ currents through ECaC and the respective mutants

Currents were measured in the absence of divalent cations at −80 mV (ramp protocol).

Mutant	Na^+ current density (pA/pF)	*n*
Nontransfected	15 ± 2	17
Wild-type	487 ± 76	16
D542A	402 ± 110	14
D542N	317 ± 55	16
D542E	46 ± 18	12
D542M	43 ± 15	17
D542K	17 ± 5	6

TABLE II

Relative permeability of monovalent cations through ECaC

Relative permeability for various monovalent cations trough ECaC as measured from reversal potential shifts (Eq. 1). Shifts were always measured from the same cells.

Mutant	K^+	Cs^+	Li^+	n^a	Type	Eisenman sequence
NT[b]	1.91 ± 0.26	1.21 ± 0.05	0.72 ± 0.04	7	K> Cs > Na> Li	IV
WT	0.59 ± 0.04	0.46 ± 0.04	0.82 ± 0.04	8	Na> Li >K >Cs	X
D542A	0.82 ± 0.06	0.73 ± 0.05	1.33 ± 0.07	8	Li>Na >K >Cs	XI
D542N	0.58 ± 0.05	0.36 ± 0.04	0.92 ± 0.07	5	Na> Li >K >Cs	X
D542E	0.75 ± 0.03	0.62 ± 0.03	1.27 ± 0.08	5	Li>Na >K >Cs	XI
D542M	2.78 ± 0.61	1.1 ± 0.07	0.71 ± 0.04	5	K> Cs > Na> Li	IV

[a] *n* = number of cells.
[b] NT, nontransfected cells; WT, wild-type ECaC.

542 by glutamate attenuated the Ca^{2+} permeability of ECaC because conserved glutamate residues form the high-affinity binding site in voltage-operated Ca^{2+} channels. The pore region of the vanilloid receptor family is homologous to ECaC but lacks the aspartate at 542, which may explain the observed low Ca^{2+} selectivity of these channels (9, 10). Instead, methionine is placed at this site. The D542M mutation in ECaC only resulted in small currents. The pore is still permeable for monovalent cations with an Eisenman type IV permeation sequence, indicating a weaker field strength binding site than that seen for all the other mutants. However, in contrast with VR1, which is permeable for Ca^{2+} and Mg^{2+}, the mutant D542M channel is impermeable for Ca^{2+}, indicating that the mechanism of permeation through the ECaC pore is different from that of VR1. It is interesting that a homologous member of this family cloned from rat intestine, calcium transporter 1, contains an additional negative aspartate between the two aspartate residues at positions 542 and 550 (16). This additional aspartate could produce subtle differences in Ca^{2+} permeability of these channels with important implications for Ca^{2+} handling in the respective tissues, but electrophysiological data about calcium transporter 1 are currently lacking to substantiate this concept.

Obviously, aspartate at position 542 is also essential for Mg^{2+} binding and channel block. In addition, Mg^{2+} block of the monovalent current through ECaC still persists when the side chain of the negatively charged residue is prolonged (D542E) or by substitution of the aspartate into the polar asparagine (D542N). Thus, the structure of the Mg^{2+}-binding site may differ from that of the Ca^{2+}-binding site. The fact that E535A increases and D550A decreases the block by Mg^{2+} indicates that Mg^{2+} binding to the essential Asp^{542} site is modulated by these adjacent negative charges.

In conclusion, the molecular determinants of Ca^{2+} selectivity and permeation of ECaC appear to reside at a single aspartate residue in the pore region, a role that is played by glutamate residues in voltage-operated Ca^{2+} channels. It is therefore tempting to speculate that the selectivity filter for Ca^{2+} in ECaC might also consist of a ring of four negatively charged residues in a tetrameric pore molecule. Consequently, single mutations in the pore of ECaC would cause defective channels, which would be unable to perform a significant Ca^{2+} absorptive function. It will certainly be challenging to search for such mutants in patients with familiar malabsorption of Ca^{2+}.

Acknowledgments—We thank Dr. J. Eggermont for providing the IRES-GFP vector and M. Crabbé, H. Van Weijenbergh, and M. Schuermans for help with the cell culture.

REFERENCES

1. Hoenderop, J. G., Vaandrager, A. B., Dijkink, L., Smolenski, A., Gambaryan, S., Lohmann, S. M., de Jonge, H. R., Willems, P. H., and Bindels, R. J. (1999) *Proc. Natl. Acad. Sci. U. S. A.* **96,** 6084–6089
2. Hoenderop, J. G., van der Kemp, A. W., Hartog, A., van de Graaf, S. *F*., van Os, C. H., Willems, P. H., and Bindels, R. J. (1999) *J. Biol. Chem.* **274,** 8375–8378
3. Hoenderop, J. G., De Pont, J. J., Bindels, R. J., and Willems, P. H. (1999) *Kidney Int.* **55,** 225–233
4. Hoenderop, J. G. J., Willems, P. H. G. M., and Bindels, R. J. M. (2000) *Am. J. Physiol.* **278,** F352–F360
5. Vennekens, R., Hoenderop, J. G.-J., Prenen, J., Stuiver, M., Willems, P. H. G. M., Droogmans, G., Nilius, B., and Bindels, R. J. M. (2000) *J. Biol. Chem.* **275,** 3963–3969
6. Nilius, B., Vennekens, R., Prenen, J., Hoenderop, J. G. J., Bindels, J. M., and Droogmans, G. (2000) *J. Physiol.* (*Lond.*) **527,** 239–248
7. Hoenderop, J. G., van der Kemp, A. W., Hartog, A., van Os, C. H., Willems, P. H., and Bindels, R. J. (1999) *Biochem. Biophys. Res. Commun.* **261,** 488–492
8. Kanzaki, M., Nagasawa, M., Kojima, I., Sato, C., Naruse, K., Sokabe, M., and Iida, H. (1999) *Science* **285,** 882–886
9. Caterina, M. J., Schumacher, M. A., Tominaga, M., Rosen, T. A., Levine, J. D., and Julius, D. (1997) *Nature* **389,** 816–824
10. Caterina, M. J., Rosen, T. A., Tominaga, M., Brake, A. J., and Julius, D. (1999) *Nature* **398,** 436–441
11. Zhu, X., and Birnbaumer, L. (1998) *News Physiol. Sci.* **13,** 211–217
12. Garcia-Martinez, C., Morenilla-Palao, C., Planells-Cases, R., Merino, J. M., and Ferrer-Montiel, A. (2000) *J. Biol. Chem.* **275,** 32552–32558
13. Trouet, D., Nilius, B., Voets, T., Droogmans, G., and Eggermont, J. (1997) *Pflügers Arch.* **434,** 632–638
14. Vennekens, R., Trouet, D., Vankeerberghen, A., Voets, T., Cuppens, H., Eggermont, J., Cassiman, J. J., Droogmans, G., and Nilius, B. (1999) *J. Physiol.* (*Lond.*) **515,** 75–85
15. Nilius, B., Oike, M., Zahradnik, I., and Droogmans, G. (1994) *J. Gen. Physiol.* **103,** 787–805
16. Hoenderop, J. G. J., Müller, D., Suzuki, M., van Os, C. H., and Bindels, R. J. M. (2000) *Curr. Opin. Nephrol. Hyperten.* **9,** 335–340
17. Ugate, G., Pérez, F., and Latorre, R. (1998) *Biol. Res.* **31,** 17–32